AD-A053 855 COLORADO STATE UNIV FORT COLLINS DEPT OF CHEMISTRY F/G 20/10
THE JAHN-TELLER EFFECT IN THE LOWEST CHARGE TRANSFER STATE OF U--ETC(U)
MAR 78 E R BERNSTEIN, G R MEREDITH, J D WEBB N00014-75-C-1179
UNCLASSIFIED TR-18 NL

END
DATE FILMED
6 -78
DDC

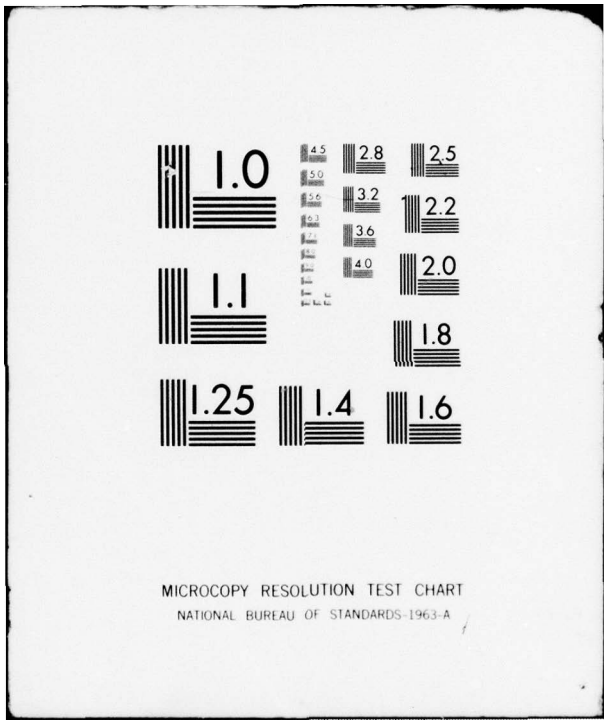
1.0
1.1
1.25
1.4
1.6
1.8
2.0
2.2
2.5
2.8
3.2
3.6
4.0
4.5
5.0
5.6
6.3
MICROCOPY RESOLUTION TEST CHART
NATIONAL BUREAU OF STANDARDS-1963-A

OFFICE OF NAVAL RESEARCH

Contract N00014-75-C-1179

Task No. NR 056-607

TECHNICAL REPORT NO. 18

"THE JAHN-TELLER EFFECT IN THE LOWEST CHARGE TRANSFER STATE OF UF_6"

by

E. R. Bernstein, G. R. Meredith and J. D. Webb

Prepared for Publication in
Journal of Chemical Physics

Department of Chemistry
Colorado State University
Fort Collins, Colorado 80523

March 1978

UNCLASSIFIED
SECURITY CLASSIFICATION OF THIS PAGE (When Data Entered)

REPORT DOCUMENTATION PAGE	READ INSTRUCTIONS BEFORE COMPLETING FORM
1. REPORT NUMBER: 18 (14) TR-18	2. GOVT ACCESSION NO. / 3. RECIPIENT'S CATALOG NUMBER
4. TITLE (and Subtitle): (6) The Jahn-Teller Effect in the Lowest Charge Transfer State of UF_6	5. TYPE OF REPORT & PERIOD COVERED: (9) Technical Report
	6. PERFORMING ORG. REPORT NUMBER
7. AUTHOR(s): (10) E. R. Bernstein, G. R. Meredith, J. D. Webb	8. CONTRACT OR GRANT NUMBER(s): (15) N00014-75-C-1179
9. PERFORMING ORGANIZATION NAME AND ADDRESS: Department of Chemistry, Colorado State University, Fort Collins, Colorado 80523	10. PROGRAM ELEMENT, PROJECT, TASK AREA & WORK UNIT NUMBERS: NR 056-607
11. CONTROLLING OFFICE NAME AND ADDRESS: Office of Naval Research, Arlington, VA 22217	12. REPORT DATE: (11) Mar 78 (12) 33 p.
	13. NUMBER OF PAGES: 35
14. MONITORING AGENCY NAME & ADDRESS (if different from Controlling Office)	15. SECURITY CLASS. (of this report): Unclassified
	15a. DECLASSIFICATION/DOWNGRADING SCHEDULE

16. DISTRIBUTION STATEMENT (of this Report)

Approved for Public Release; Distribution Unlimited.

17. DISTRIBUTION STATEMENT (of the abstract entered in Block 20, if different from Report)

18. SUPPLEMENTARY NOTES

19. KEY WORDS (Continue on reverse side if necessary and identify by block number)

Uranium hexafluoride
Emission
Charge transfer states
Jahn-Teller Effect
Vibronic coupling
Three-dimensional harmonic oscillator
Franck-Condon envelope

20. ABSTRACT (Continue on reverse side if necessary and identify by block number)

The neat and mixed crystal emission spectra of UF_6 are analyzed. It is found that long uniquantal progressions appear in the ν_5 (t_{2g}) vibration built on the origin, ν_6 (t_{2u}), and $n_1\nu_1$ (a_{1g}). The maximum intensity in all

DD FORM 1 JAN 73 1473 EDITION OF 1 NOV 65 IS OBSOLETE
S/N 0102-014-6601

UNCLASSIFIED
SECURITY CLASSIFICATION OF THIS PAGE (When Data Entered)

404 992

20. (continued...)

these series falls around $n_5 = 2$. These data are interpreted as being indicative of a substantial molecular Jahn-Teller interaction in the excited charge transfer state. Using a modified Franck-Condon analysis for a 3-dimensional vibrational space, it is found that $D_{(5)}^{*} \approx 2.02$ and that the excited state is distorted along each of three ν_5 coordinates by roughly 0.09 Å.

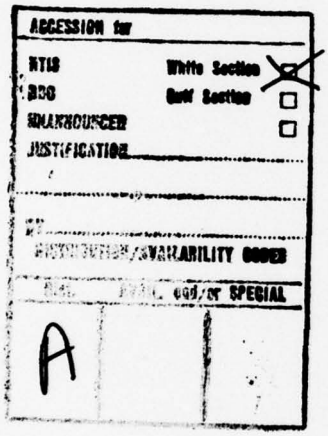

* is approx.

I. INTRODUCTION

Interest in the charge-transfer (CT) states of metal hexahalides has been increasing in recent years due to advances in both theoretical and experimental techniques (1-3). Xα calculational methods have shown good promise for obtaining at least a qualitative understanding of these many-electron systems. Careful absorption and emission studies of CT systems have, moreover, demonstrated a surprising degree of detail that had previously gone unnoticed.

Transfer of an electron to a central metal orbital from a bonding ligand orbital often results in a series of degenerate electronic states. In the bonding electronic structure, such degeneracy can lead to substantial Jahn-Teller (JT) interactions and even static distortions. It has proved difficult to study large JT effects in ground state molecules as they tend to remove the system permanently from high symmetry. Thus, molecules with accessible CT states are of particular interest in this regard. Transition metal hexafluorides have been successfully used in the past to study weak JT effects within the 4d and 5d electronic manifolds (4). Almost all of these molecules exhibit resolvable CT spectra; they are thereby an appropriate vehicle for the study of strong JT interactions involving bonding electrons. Associated with the JT effect are the more general problems of radiationless transitions and vibronic coupling. The work reported herein is a first step toward dealing with these larger concerns.

UF_6 is known to emit from its lowest charge-transfer state, and thus is a good candidate for study. The emission spectrum of neat UF_6 at 77 K has been reported (5a,5b); however, the observed spectra are so diffuse that it is impossible to make detailed assignments and draw useful conclusions. The work reported here improves on this situation by taking the emission spectrum of neat UF_6 at a lower temperature, 1.6 K, and also by employing a mixed crystal,

5% UF_6/WF_6. The latter sample eliminates exciton interactions which tend to broaden features in the spectrum.

Since the results of these experiments suggest a Jahn-Teller interaction in the excited state, Sec. II deals mainly with an approximate method for determining the magnitude of the Jahn-Teller interaction in a state given its emission spectrum to an A_{1g} state. Franck-Condon overlap integrals for three-dimensional harmonic oscillators are required for this approximate technique, but are not readily available, thus they are also worked out in Sec. II.

Data from both pure and mixed crystals are presented in Sec. IV, since both are helpful in making assignments and in understanding the overall spectrum.

II. THEORY

A. Three-Dimensional Harmonic Oscillator Franck-Condon Overlap Integral

The appearance of a uniquantal progression in the triply degenerate ν_5 (t_{2g}) mode in the UF_6 emission spectrum provides motivation to find the expression for the Franck-Condon overlap integral

$$J(^{0}_{n_\xi}\,^{0}_{n_\eta}\,^{0}_{n_\zeta}) = \int_{-\infty}^{\infty}\int\int \psi^{II}_{000}(q_\xi,q_\eta,q_\zeta)\ \psi^{I}_{n_\xi n_\eta n_\zeta}(q_\xi,\ q_\eta,\ q_\zeta)\ dq_\xi dq_\eta dq_\zeta. \tag{1}$$

The function ψ^{II}_{000} represents the ν_5 vibrational contribution to the excited state zero point wave function, while $\psi^{I}_{n_\xi n_\eta n_\zeta}$ is the function for any ν_5 vibration in the ground state manifold. The coordinate system has its origin at the equilibrium octahedral configuration of the ground state. Thus, the ψ^{I} functions are just harmonic oscillator functions, whereas ψ^{II} functions are not, but can be related to them.

The three-dimensional harmonic oscillator wavefunction in Cartesian coordinates can be written as follows:

$$\psi^{I}_{n_\xi n_\eta n_\zeta}(q_\xi,\ q_\eta,\ q_\zeta) = N_{n_\xi n_\eta n_\zeta}\ e^{-\frac{\gamma}{2}(q_\xi^2 + q_\eta^2 + q_\zeta^2)}$$
$$\times\ H_{n_\xi}(\gamma^{1/2}q_\xi)\ H_{n_\eta}(\gamma^{1/2}q_\eta)\ \ H_{n_\zeta}(\gamma^{1/2}q_\zeta). \tag{2}$$

in which

$$N_{n_\xi n_\eta n_\zeta} = \left(\frac{\gamma^{3/2}}{\pi^{3/2}\ 2^{n_\xi + n_\eta + n_\zeta}\ n_\xi!\ \ n_\eta!\ \ n_\zeta!} \right)^{1/2}, \qquad \gamma = \frac{\mu_\tau\ \omega_\tau}{\hbar},$$

μ_τ is the reduced mass, and $H_n(\gamma^{1/2}q)$ is a Hermite polynomial.

The wave function can be put in a more useful form using the relations

$$Q_i = \gamma^{\frac{1}{2}} q_i \qquad i = \xi, \eta, \zeta \tag{3}$$

and

$$H_n(Q) = (-1)^n e^{Q^2} \frac{d^n e^{-Q^2}}{dQ^n} \quad . \tag{4}$$

thus

$$\psi^{I}_{n_\xi n_\eta n_\zeta}(q_\xi, q_\eta, q_\zeta) = N_{n_\xi n_\eta n_\zeta} \prod_{i=\xi,\eta,\zeta} (-1)^{n_i} e^{\frac{Q_i^2}{2}} \frac{d^{n_i} e^{-Q_i^2}}{dQ_i^{n_i}} \quad . \tag{5}$$

The vibrational wave function for the emitting state can be expressed in terms of ground state functions

$$\psi^{II}_{ooo}(q_\xi, q_\eta, q_\zeta) = \psi^{I}_{ooo}(q_\xi + q^o_\xi, q_\eta + q^o_\eta, q_\zeta + q^o_\zeta) \tag{6}$$

in which $(q^o_\xi, q^o_\eta, q^o_\zeta)$ are the relative distortion parameters of the excited state; i.e., the shift in the origin of the ν_5 vibrational coordinates upon excitation. With the above expressions, eq. (1) can be solved in general using integration by parts. $J^2\left(\begin{smallmatrix} o & o & o \\ n_\xi & n_\eta & n_\zeta \end{smallmatrix}\right)$, the quantity useful in determining transition intensities, is given by the relation

$$J^2\left(\begin{smallmatrix} o & o & o \\ n_\xi & n_\eta & n_\zeta \end{smallmatrix}\right) = \frac{e^{-\{P^o_\xi + P^o_\eta + P^o_\zeta\}} (P^o_\xi)^{n_\xi} (P^o_\eta)^{n_\eta} (P^o_\zeta)^{n_\zeta}}{n_\xi!\ n_\eta!\ n_\zeta!} \tag{7}$$

with

$$P^o_i = Q^{o\,2}_i / 2$$

$$Q^o_i = \gamma^{\frac{1}{2}} q^o_i \qquad i = \xi, \eta, \zeta \quad .$$

It should be noted that this expression does not take into account frequency differences of the ν_5 vibration in the ground and excited states. However,

it has been shown that for the case of vibrations with a common origin, unless the frequency difference is very large, little intensity occurs outside the 0-0 (6,7).

In this case, the intensity of any peak relative to the origin transition is the relevant quantity; it is given by the following expression:

$$K_{n_\xi n_\eta n_\zeta} = \frac{J^2\begin{pmatrix} 0 & 0 & 0 \\ n_\xi & n_\eta & n_\zeta \end{pmatrix}}{J^2\begin{pmatrix} 0 & 0 & 0 \\ 0 & 0 & 0 \end{pmatrix}} = \frac{(P_\xi^0)^{n_\xi}\,(P_\eta^0)^{n_\eta}\,(P_\zeta^0)^{n_\zeta}}{n_\xi!\;\; n_\eta!\;\; n_\zeta!} \quad . \tag{8}$$

The relative transition intensity to a degenerate level n, W_n, is the sum of the individual contributions

$$W_n = \sum_{n_\xi + n_\eta + n_\zeta = n} K_{n_\xi n_\eta n_\zeta}. \tag{9}$$

Figure 1 graphically presents some Franck-Condon progressions based on eq. 9 for various P^0, in the case $P^0 = P_\xi^0 = P_\eta^0 = P_\zeta^0$. Of course, these curves are similar to the more familiar one-dimensional case.

B. Intensity Pattern of a $T_{ig} \rightarrow A_{1g}$ Transition for a $T_{ig} \times t_{2g}$ Static Jahn-Teller System.

The appearance of ν_5 progressions in the UF_6 emission spectrum suggests a JT interaction in the excited state. Methods for relating this information to JT parameters are discussed in this section.

The vibronic Hamiltonian for a linear $T_{ig} \times t_{2g}$ (i = 1,2) JT system is

$$\underline{\mathscr{H}}^{\tau} \sim \underline{\mathscr{H}}_0^{\tau} + \underline{\mathscr{H}}_1^{\tau} \tag{10}$$

$$\underline{\mathscr{H}}_0^{\tau} = \frac{1}{2\mu_\tau} \left\{ (\hat{P}_\xi^2 + \hat{P}_\eta^2 + \hat{P}_\zeta^2) + \mu_\tau^2 \omega_\tau^2 (q_\xi^2 + q_\eta^2 + q_\zeta^2) \right\} \underline{I}$$

$$\underline{\mathscr{H}}_1^{\tau} = \ell_\tau (q_\xi \underline{\tau}_1 + q_\eta \underline{\tau}_2 + q_\zeta \underline{\tau}_3)$$

in which ℓ_τ is the linear coupling coefficient and $\underline{\tau}_i$ are 3 x 3 matrices given by Moffitt and Thorson (8). Information on the JT effect in such an excited state system can be obtained either by direct observation of the JT state in absorption ($T_{ig} \leftarrow A_{1g}$) or by emission ($T_{ig} \rightarrow A_{1g}$). In the latter case, the vibronic information is contained in the t_{2g} progression intensity and its distribution. The rigorous method within the linear approximation for calculating relative intensities of a ν_5 progression in $T_{ig} \rightarrow A_{1g}$ transitions is to solve the full secular matrix for the T_{ig} state (9,10). Coefficients in the eigenvector for the lowest energy state can then be used to give the desired transition probabilities. The linear JT parameter can be varied until the calculated intensities match the observed ones. However, examination of calculated ν_5 intensities (10) suggests a more simple, although more approximate, approach, in that

the intensity pattern resembles a Franck-Condon progression. In this method, the observed pattern is duplicated as closely as possible by a Franck-Condon progression, and the Franck-Condon parameter is used to find the distortion in the JT state. In linear JT theory the distortion can be easily related to the JT stabilization energy, E_{JT}. It is expected that this approximation will improve as E_{JT} increases; dynamic effects involving the various potential surfaces decrease (8) as the distortion becomes predominant.

Substitution of the Franck-Condon approach for the more exact but cumbersome linear JT calculation of the emission intensity is straightforward and the details of this approximation are briefly presented here. Eq. 9 is used as the starting point; it gives the intensities as a function of the distortion parameters, $\{P_i^o\}$.

The distorted geometry and general surface topology of a $T_{ig} \times t_{2g}$ JT molecule are well known (8). The conditions for minima in the potential energy surfaces are

$$| q_\xi^o | = | q_\eta^o | = | q_\zeta^o |, \tag{11}$$

$$q_\xi^o \, q_\eta^o \, q_\zeta^o = -\Delta^3,$$

and

$$\Delta = \frac{2}{3} \frac{\ell_\tau}{\mu_\tau \omega_\tau^2}$$

which corresponds to a trigonal distortion. The equality of the three distortion parameters leads to a considerable simplification of Eq. 9

$$W_n = \frac{(3 P^o)^n}{n!} \tag{12}$$

for which

$$P^o = P_\xi^o = P_\eta^o = P_\zeta^o .$$

The relation between the radial distortion, q_r^o, and E_{JT} can be found by noting that

$$q_r^o = \sqrt{q_\xi^{o\,2} + q_\eta^{o\,2} + q_\zeta^{o\,2}} = \sqrt{3}\,\Delta = \frac{2\sqrt{3}}{3}\,\frac{\ell_\tau}{\mu_\tau \omega_\tau^{\,2}}\,, \tag{13}$$

$$E_{JT} = \frac{2}{3}\,\frac{\ell_\tau^{\,2}}{\mu_\tau \omega_\tau^{\,2}}\,. \tag{14}$$

Equations 13 and 14 can be solved to give

$$E_{JT} = \frac{1}{2}\,\mu_\tau \omega_\tau^{\,2}\, q_r^{o\,2} \tag{15}$$

or in dimensionless quantities

$$D_5 = \frac{\ell_\tau^{\,2}}{2\hbar\mu_\tau\omega_\tau^{\,3}} = \frac{E_{JT}}{(4/3)\hbar\omega_\tau} = \frac{3}{8}\left(\frac{\mu_\tau\omega_\tau}{\hbar}\right) q_r^{o\,2} = \frac{3}{8}\{Q_\xi^{o\,2} + Q_\eta^{o\,2} + Q_\zeta^{o\,2}\} = \frac{9}{4}\,P^o\,. \tag{16}$$

The Franck-Condon intensities can then be expressed directly in terms of D_5

$$W_n = \frac{(\frac{4}{3}\,D_5)^n}{n!}\,. \tag{17}$$

The approximation can be tested by attempting to fit a progression calculated by the secular matrix method (10) and comparing the resulting parameter with the known value. This is illustrated in Figure 2 where the curve with the known parameter, k = 2.3 (10) (D_5 = 2.64), is fit reasonably well by a Franck-Condon progression giving D_5 = 2.32. Thus the approximate technique comes within 15% of the rigorous method.

It should be noted that this approach has difficulties for some other linear JT problems such as $E_g \times e_g$ (6) or $G_{3/2g} \times t_{2g}$ (8) due to their accidental high vibronic symmetries (cylindrical and spherical, respectively).

III. EXPERIMENTAL

The hexafluoride samples (5% UF_6/WF_6, 0.3% ReF_6/UF_6) were prepared by previously reported techniques (11). The .3% ReF_6/UF_6 can be considered a neat UF_6 crystal since the 0.3% ReF_6 dopant does not appreciably disturb the translational symmetry of the lattice, and ReF_6 itself does not emit in the visible region (12). It probably does weaken the UF_6 emission by acting as a deep trap, but this does not create any essential difficulties. The experimental set-up for measuring the emission spectrum consisted of a UV Ar^+ laser, pre-disperser, optical dewar, and double-1/2 meter monochromator, a cooled photo-multiplier tube (either RCA C31034A or RCA 8850) and photon counting equipment. Typical slit widths were 0.16 Å. The laser power used for the 5% UF_6/WF_6 sample was 10 mW of 3638 Å, whereas the 0.3% ReF_6/UF_6 sample required 500 mW of all the UV Ar^+ laser lines.

Calibration was achieved by recording a number of Fe-Ne standard lines (13) over the range of the emission spectrum and fitting a least-squares curve designed to account for a cam action in the drive mechanism of the monochromator as well as a slight curvature in the correction function.

IV. RESULTS AND DISCUSSION

Frequencies and assignments for the emission spectra of 5% UF_6/WF_6 and neat UF_6 (.3% ReF_6/UF_6) are given in Tables 1 and 2. Figures 3 and 4 present tracings of the spectra.

The 5% UF_6/WF_6 emission spectrum has two dominant characteristics: several ν_5 (t_{2g}) progressions and intense phonon side bands. The phonons are primarily built on the origin and ν_5 peaks; they cause a high underlying background intensity, obscuring weaker transitions and contribute to the apparent broadening of many features. Additionally, there is also a much weaker progression in the totally symmetric ν_1 which is indicative of a change in bond length in the excited state. ν_2, ν_3, ν_4 are conspicuous by their absence.

The neat UF_6 emission spectrum appears superficially quite different: the $n\nu_1$ progression is more obvious while the $n\nu_5$ progressions quickly broaden and blend into the background intensity, the phonons do not dominate the vibronic part of the spectrum, ν_6 is more intense, and ν_4 is observed. The important question is whether these differences are due to site effects, which might change the geometries of the ground and excited states, or other phenomena such as excitons.

A consistent picture arises concerning the differences between neat and mixed crystal UF_6 spectra (compare Figures 3 and 4) if one considers exciton effects in both the emitting and ground vibrational states and phonons built on these exciton bands (14). The neat crystal emission spectra are characterized by band-to-band transitions due to thermalization in the upper exciton state. Thus the neat crystal $n\nu_5$ bands are quite broad (60 cm^{-1}), the ν_6 band is relatively sharp (18 cm^{-1}) and the $n\nu_1$ series is the sharpest observed (~10

cm^{-1}) as would be expected from the ground state vibrational spectra. On the other hand, in the mixed crystal, ν_5 is the sharpest vibronic feature (20 cm^{-1}) as ν_1 is obscured and/or broadened by ($3\nu_5$ + phonons). These latter phonon modes play an important role in mixed crystal spectra but only a minor one in pure crystal spectra. Apparent differences are particularly obvious for the ν_1 progression. Since ν_1 is a localized exciton mode ($\Delta\ \nu_1 < 1.0\ cm^{-1}$ (14)) it does not interact strongly with the highly delocalized exciton plus phonon structure of the neat crystal. The appearance of ν_4 in the neat, but not in the mixed, crystal spectrum might be due to differences in the Fermi resonance interaction in the neat and mixed crystal situations.

The most interesting aspect of the spectrum is the appearance of a number of long ν_5 progressions. The uniquantal nature of the progressions proves that they are due to a t_{2g} distortion in the excited state and not simply a large ν_5 frequency shift. The cause of the distortion is, however, not as certain. There are three possibilities for the excited state change in geometry:

1. The nature of the excited state electronic wave function is such that a D_{3d} geometry is preferred. One can refer to this case simply as *electronic distortion.* However, too little is known about charge-transfer states in the hexafluorides for a careful assessment of the plausibility of this mechanism.
2. The low crystal site symmetry (C_s) imposes the distortion on the molecule. However, this appears to be unlikely: the distortion $O_h \rightarrow C_s$ would then involve other coordinates besides t_{2g} (additional progressions would be expected) and both neat and mixed crystal spectra have their $n\nu_5$ progression maxima at n = 2. In order that the site symmetry be responsible for the distortion,

UF_6 must be very sensitive to small site perturbations. We have previously shown that the sites in UF_6 and WF_6 are somewhat different (14), and thus the similarity of the spectra mitigates against this possibility for the distortion mechanism.

3. A strong Jahn-Teller effect causes the t_{2g} distortion. Theoretical calculations predict that the lowest excited states of UF_6 are degenerate and would, because of their CT nature, be particularly susceptible to a substantial JT distortion. The absorption spectrum of the emitting state should, in principle, reveal whether a JT effect is present or not, but its complexity and congestion has thus far limited its usefulness. Nonetheless, a JT effect is not inconsistent with the absorption data; peaks are observed at [origin + 169 cm^{-1}] and [origin + 202 cm^{-1}]. We suggest these are the JT split ν_5 components to be expected for a strong intrastate vibronic interaction and an unperturbed ν_5^0 of 205 cm^{-1} (8,10).

Of the three proposed mechanisms for inducing long ν_5 progressions, the JT effect seems the most likely, and will be assumed in the following data analysis. It should be kept in mind, however, that the trigonal distortion parameter P^o is independent of mechanistic assumptions.

Intensity data for the ν_5 progressions from both the neat and mixed crystal spectra are not as good as one might like. The neat crystal data have difficulties with broad, overlapping exciton bands, while the mixed crystal spectra suffer from underlying phonon intensity. However, the mixed crystal data are better and will be used here.

The approximate theory necessary to treat the ν_5 intensity data is presented in Section III. Only the $T_{ig} \times t_{2g}$ linear JT theory is treated as the other degenerate state symmetry, E_g, has no JT interaction with a t_{2g} vibra-

tion (8). Thus the emitting state is either of T_{1g} or T_{2g} symmetry.

Table 3 gives a comparison of observed and calculated relative intensities for the $n\nu_5$ and $\nu_6 + n\nu_5$ progressions. The calculations use either Eq. 12 or 17. It is interesting that the intensity patterns for the $n\nu_5$ and $\nu_6 + n\nu_5$ progression are different, thus leading to different parameter values. Since both patterns are fit well by Franck-Condon curves, it seems reasonable to attribute the difference to the vibronic nature of the ν_6 false origin. Brand and Goodman (15) have shown that JT progressions built on vibronically allowed transitions can be strongly influenced by the JT nature of the vibronically coupled donor states. Thus, the parameters derived from the $\nu_6 + n\nu_5$ progression ($D_5 = 1.40$, $P^o = 0.62$) are probably less meaningful in the present context than are those for $n\nu_5$ ($D_5 = 2.02$, $P^o = 0.9$). The $P^o = 0.9$ corresponds to a trigonal distortion with $|q^o_\xi| = |q^o_\eta| = |q^o_\zeta| = 0.09$ Å.

Early work on the luminescence of neat UF_6 at 88 K (5b) indicated a ~20 member progression with a ~200 cm^{-1} interval. That observation can be reconciled with the present data by noting several near resonances: for example, $(3n + m)\ \nu_5 \sim (n\nu_1 + m\nu_5)$ and $(n\nu_1 + \nu_6 + m\nu_5) \sim (3n + m + 1)\nu_5$. Thus the previously assigned 20th member of the progression is not $20\nu_5$ but rather more likely $5\nu_1 + \nu_6 + 4\nu_5$.

V. CONCLUSIONS

Strong emission from UF_6 crystals (neat UF_6 or 5% UF_6/WF_6) from ~4100 Å - 4800 Å has been observed. Differences between the two spectra are due mainly to differences between localized (5% UF_6/WF_6) and delocalized exciton states (neat UF_6). The appearance of several long uniquantal ν_5 (t_{2g}) progressions in the spectrum is proof that the emitting state is distorted, relative to the ground state, along the ν_5 coordinates. The cause of the distortion is tentatively identified as a strong Jahn-Teller interaction (D_5 ~2.02). The distortion of the excited state thus turns out to be about 0.09 Å in each of the ν_5 coordinates.

ACKNOWLEDGEMENT

During the final stages of preparation of this manuscript we received a preprint from L. Andrews on emission of UF_6 in argon matrices. The data presented therein are in substantial agreement with those discussed here. We thank Professor Andrews for sending us his manuscript and for helpful conversations about his results.

REFERENCES

1. W. B. Lewis, L. B. Asprey, L. H. Jones, R. S. McDowell, S. W. Rabideau, A. H. Zeltman and R. T. Paine, J. Chem. Phys. 65, 2707 (1976).

2. J. C. Collingwood, S. B. Piepho, R. W. Schwartz, P. A. Dobosh, J. R. Dickinson and P. N. Schatz, Mol. Phys. 29, 793 (1975).

3. R. McDiarmid, J. Chem. Phys. 61, 3333 (1974).

4. G. R. Meredith, J. D. Webb and E. R. Bernstein, Mol. Phys., in press (and references therein).

5a. Dieke and Duncan, Spectroscopic Properties of Uranium Compounds, (McGraw-Hill, New York, 1949), Ch. 8.

b. G. D. Sheremet'ev, Optika i Spektroskopiya 2, 99 (1957).

6. H. C. Longuet-Higgins, U. Opik, M.H.L. Pryce, F.R.S. and R. A. Sack, Proc. Roy. Soc. (London) 244 A, 1 (1958).

7. G. Herzberg, Electronic Spectra of Polyatomic Molecules, (D. van Nostrand, New York, 1966), p. 150.

8. W. Moffitt and W. Thorson, Phys. Rev. 108, 1251 (1957).

9. M. Caner and R. Englman, J. Chem. Phys. 44, 4054 (1966).

10. R. Englman, M. Caner and S. Toaff, J. Phys. Soc. Japan 29, 306 (1970).

11. E. R. Bernstein and G. R. Meredith, J. Chem. Phys. 64, 375 (1976).

12. G. R. Meredith, Ph.D. Thesis, Princeton University, 1977.

13. H. M. Crosswhite, J. Res. Nat. Bureau Std. 79A, 17 (1975).

14. E. R. Bernstein and G. R. Meredith, Chem. Phys. 24, 289, 301, 311 (1977).

15. J. C. D. Brand and G. L. Goodman, Can. J. Phys. 46, 1721 (1968).

Table 1. The emission spectrum of 5% UF_6/WF_6 at 1.6 K with 0.16 Å slits and 10 mW of 3638 Å laser power from a UV Ar^+ laser. The absolute wavelength calibration is ±0.04 Å (standard deviation).

λ_{Air}(Å)	σ_{Vacuum}(cm^{-1})	FWHH[a] (cm^{-1})	I	$\Delta\sigma$(cm^{-1})	Assignment
4065.39	24590.9	12	1[b]	0	Origin
4067.22	24579.9			11.1	Phonon a
4070.57	24559.6	35	1[c]	31.3	Phonon b
4076.89	24521.6			69.4	Phonon c
4081.92	24491.4			99.6	Phonon d
4092.59	24427.5	28	1[d]	163.4	ν_6
4099.67	24385.3	20	2.85[b]	205.6	ν_5
4104.90	24354.3	30	2.36[c]	236.7	ν_5 + phonon b
4110.87	24318.9			272.1	ν_5 + phonon c
4117.02	24282.6			308.4	ν_5 + phonon d
4127.42	24221.4	27	1.70[d]	369.6	$\nu_6 + \nu_5$
4131.71	24196.2			394.7	$\nu_6 + \nu_5$ + phonon b
4134.41	24180.4	28	3.75[b]	410.5	$2\nu_5$
4139.88	24148.5		3.20[c]	442.5	$2\nu_5$ + phonon b
4145.76	24114.2			476.7	$2\nu_5$ + phonon c
4152.06	24077.6			513.3	$2\nu_5$ + phonon d
4162.38	24017.9	28	1.70[d]	573.0	$\nu_6 + 2\nu_5$
4167.26	23989.8			601.1	$\nu_6 + 2\nu_5$ + phonon b
4169.82	23975.1	38	3.25[b]	615.8	$3\nu_5$
4175.23	23944.0		2.76[c]	646.9	$3\nu_5$ + phonon b
4178.82	23923.5	12		667.5	ν_1
4183.79	23895.0			695.9	ν_1 + phonon b
4188.18	23870.0			720.9	$3\nu_5$ + phonon d
4198.42	23811.8	26	1.1[d]	779.2	$\nu_6 + 3\nu_5$
4205.79	23770.0	50	2.85[b]	820.9	$4\nu_5$
4207.44	23760.7			830.2	$\nu_1 + \nu_6$
4211.49	23737.9			853.1	$4\nu_5$ + phonon b
4214.88	23718.8	12		872.2	$\nu_1 + \nu_5$
4220.15	23689.2			901.8	ν_1 + phonon b
4225.06	23661.6			929.3	ν_1 + phonon c; $4\nu_5$ + phonon d

Table 1. (cont'd.)

λ_{Air}(Å)	σ_{Vacuum}(cm^{-1})	FWHH[a] (cm^{-1})	I	$\Delta\sigma$(cm^{-1})	Assignment
4234.9	23606.7	27	0.59[d]	984.3	$\nu_6 + 4\nu_5$
4242.52	23564.3	42	2.60[b]	1026.7	$5\nu_5$
4244.08	23555.6			1035.3	$\nu_1 + \nu_6 + \nu_5$
4249.3	23526.7			1064.3	$5\nu_5$ + phonon b
4251.54	23514.3			1076.7	$\nu_1 + 2\nu_5$
4257.09	23483.6			1107.3	$\nu_1 + 2\nu_5$ + phonon b
4271.55	23404.7		0.18[d]	1186.8	$\nu_6 + 5\nu_5$
4279.54	23360.4			1230.5	$6\nu_5$
4281.17	23351.5			1239.4	$\nu_1 + \nu_6 + 2\nu_5$
4286.31	23323.5			1267.4	$6\nu_5$ + phonon b
4288.98	23309.0			1281.9	$\nu_1 + 3\nu_5$
4292.36	23290.7			1300.3	$6\nu_5$ + phonon c
4295.08	23275.9			1315.0	$\nu_1 + 3\nu_5$ + phonon b
4298.35	23258.2			1332.7	$2\nu_1$
4309.52	23197.9			1393.0	$\nu_6 + 6\nu_5$
4319.02	23146.9			1444.1	$\nu_1 + \nu_6 + 3\nu_5$
4326.82	23105.2			1485.8	$\nu_1 + 4\nu_5$
4332.47	23075.0			1515.9	$\nu_1 + 4\nu_5$ + phonon b
4336.44	23053.9			1537.0	$2\nu_1 + \nu_5$
4357.89	22940.4			1650.5	$\nu_1 + \nu_6 + 4\nu_5$
4365.78	22899.0			1692.0	$\nu_1 + 5\nu_5$
4372.47	22863.9			1727.0	$\nu_1 + 5\nu_5$ + phonon b
4375.8	22846.5			1744.4	$2\nu_1 + 2\nu_5$
4396.86	22737.1			1853.8	$\nu_1 + \nu_6 + 4\nu_5$
4406.45	22687.6			1903.3	$\nu_1 + 6\nu_5$; $2\nu_1 + \nu_6 + 2\nu_5$
4411.30	22662.7			1928.3	$\nu_1 + 6\nu_5$ + phonon b
4415.5	22641.1			1949.8	$2\nu_1 + 3\nu_5$
4436.95	22531.7			2059.3	$\nu_1 + \nu_6 + 6\nu_5$
4446.8	22481.8			2109.2	$\nu_1 + 7\nu_5$; $2\nu_1 + \nu_6 + 3\nu_5$
4454.72	22441.8			2149.1	$2\nu_1 + 4\nu_5$
4483.3	22273.7			2317.2	$2\nu_1 + \nu_6 + 4\nu_5$
4497.3	22229.2			2361.8	$2\nu_1 + 5\nu_5$
4502.7	22202.8			2388.1	$2\nu_1 + 5\nu_5$ + phonon b

Table 1. (cont'd.)

λ_{Air}(Å)	σ_{Vacuum}(cm^{-1})	FWHH[a] (cm^{-1})	I	$\Delta\sigma$(cm^{-1})	Assignment
4529.7	22070.5			2520.5	$2\nu_1 + \nu_6 + 5\nu_5$
4539.3	22023.5			2567.4	$2\nu_1 + 6\nu_5$
4545.3	21994.4			2596.5	$2\nu_1 + 6\nu_5$ + phonon a
4571.3	21869.3			2721.6	$2\nu_1 + \nu_6 + 6\nu_5$
4582.3	21816.8			2774.1	$2\nu_1 + 7\nu_5$
4591.0	21775.6			2815.3	$3\nu_1 + 4\nu_5$
4625.3	21614.0			2976.9	$2\nu_1 + 8\nu_5$
4634.7	21570.3			3020.7	$3\nu_1 + 5\nu_5$
4670.0	21407.4			3183.5	$2\nu_1 + 9\nu_5$
4679.3	21364.7			3226.2	$3\nu_1 + 6\nu_5$
4724.7	21159.7			3431.2	$3\nu_1 + 7\nu_5$
4734.0	21117.9			3473.0	$3\nu_1 + 7\nu_5$ + phonon b; $4\nu_1 + 4\nu_5$
4771.3	20952.7			3638.2	$3\nu_1 + 8\nu_5$
4781.3	20908.8			3682.1	$3\nu_1 + 8\nu_5$ + phonon b; $4\nu_1 + 5\nu_5$

(a) FWHH = full width at half height.

(b) Intensity relative to origin. Baseline is approximated as underlying envelope due to phonon intensity (see Figure 3).

(c) Intensity measured relative to phonon b in similar manner to (b).

(d) Intensity measured relative to ν_6 in similar manner to (b).

Table 2. Emission spectrum of neat UF_6 at 1.6 K. The excitation source was 500 mW from a UV Ar^+ laser. The slitwidth of the monochromator corresponds to 0.16 Å. Due to the large linewidths of most of the observed peaks, the absolute wavelength is only calibrated to ±2.0 Å, but wavelength differences between peaks for the sharper lines are much better, ±0.2 Å.

λ_{Air}(Å)	σ_{Vacuum}(cm^{-1})	$\Delta\sigma$ (cm^{-1})	Assignment
4068.4	24572.7	0.0	Origin
4074.3	24537.2	35.6	Phonon a
4080.8	24498.1	74.7	Phonon b
4093.4	24422.7	150.1	
4093.9	24419.7	153.1	ν_6
4095.3	24411.3	161.4	
4097.7	24397.0	175.7	ν_4
4099.6	24385.7	187.0	
4101.1	24376.8	195.9	
4102.2	24370.3	202.5	
4104.1	24359.0	213.7	ν_5
4105.3	24351.9	220.9	
4110.2	24322.9	249.9	ν_5 + phonon a
4120.0	24265.0	307.8	$2\nu_6$
4125.4	24233.2	339.5	$\nu_4 + \nu_6$ (?)
4127.8	24219.1	353.6	$2\nu_4$
4129.9	24206.8	365.9	
4131.0	24200.4	372.4	$\nu_6 + \nu_5$
4133.6	24185.2	387.6	$\nu_4 + \nu_5$
4135.4	24174.6	398.1	
4136.2	24170.0	402.8	$2\nu_5$
4138.4	24157.1	415.6	
4139.6	24150.1	422.6	
4142.1	24135.5	437.2	$2\nu_5$ + phonon a
4166.8	23992.5	580.3	$\nu_6 + 2\nu_5$
4172.2	23961.4	611.3	$3\nu_5$
4181.4	23908.7	664.1	ν_1
4187.7	23872.7	700.0	ν_1 + phonon a
4195.0	23831.2	741.6	ν_1 + phonon b
4202.6	23788.1	784.7	$\nu_6 + 3\nu_5$

Table 2. (cont'd.)

λ_{Air}(Å)	σ_{Vacuum}(cm^{-1})	$\Delta\sigma$ (cm^{-1})	Assignment
4208.2	23756.4	816.3	
4208.8	23753.0	819.7	$\nu_1 + \nu_6$
4209.9	23746.8	825.9	
4212.5	23732.2	840.6	$\nu_1 + \nu_4$
4213.9	23724.3	848.4	$4\nu_5$
4214.5	23720.9	851.8	
4215.9	23713.0	859.7	
4217.4	23704.6	868.1	
4219.4	23693.4	879.3	$\nu_1 + \nu_5$
4220.7	23686.1	886.7	
4221.5	23681.6	891.2	$\nu_1 + 2\nu_6$
4236.2	23599.4	973.6	$\nu_1 + \nu_6 + \nu_4$ (?)
4241.4	23570.5	1002.3	$\nu_6 + 4\nu_5$
4244.4	23553.8	1018.9	
4247.3	23537.7	1035.0	$\nu_1 + \nu_6 + \nu_5$
4250.4	23520.6	1052.2	$5\nu_5$
4253.1	23505.4	1067.3	
4284.5	23333.4	1239.4	$\nu_1 + \nu_6 + 2\nu_5$
4301.0	23243.9	1328.9	$2\nu_1$
4322.0	23130.9	1441.8	$\nu_1 + \nu_6 + 3\nu_5$
4328.8	23094.6	1478.2	$2\nu_1 + \nu_6$
4335.4	23059.4	1513.3	$\nu_1 + 4\nu_5$; $2\nu_1 + \nu_4$
4337.8	23046.7	1526.1	
4340.4	23032.9	1539.9	$2\nu_1 + \nu_5$
4341.6	23026.5	1546.2	
4358.8	22935.6	1637.1	$2\nu_1 + \nu_6 + \nu_4$ (?)
4364.0	22908.3	1664.4	$\nu_1 + \nu_6 + 4\nu_5$
4369.6	22879.0	1693.8	$2\nu_1 + \nu_6 + \nu_5$
4408.8	22675.5	1897.2	$2\nu_1 + \nu_6 + 2\nu_5$
4426.8	22583.3	1989.4	$3\nu_1$
4449.6	22467.6	2105.1	$2\nu_1 + \nu_6 + 3\nu_5$
4457.0	22430.0	2142.4	$3\nu_1 + \nu_6$
4465.2	22389.1	2183.6	$2\nu_1 + 4\nu_5$

Table 2. (cont'd.)

λ_{Air}(Å)	σ_{Vacuum} (cm^{-1})	$\Delta\sigma$ (cm^{-1})	Assignment
4470.0	22365.1	2207.7	$3\nu_1 + \nu_5$
4499.8	22217.0	2355.8	$3\nu_1 + \nu_6 + \nu_5$
4540.6	22020.4	2552.3	$3\nu_1 + \nu_6 + 2\nu_5$
4560.8	21919.8	2652.9	$4\nu_1$
4584.6	21806.0	2766.7	$3\nu_1 + \nu_6 + 3\nu_5$
4592.0	21770.9	2801.8	$4\nu_1 + \nu_6$
4637.6	21556.8	3015.9	$4\nu_1 + \nu_6 + \nu_5$
4681.0	21357.0	3215.8	$4\nu_1 + \nu_6 + 2\nu_5$
4702.6	21258.9	3313.9	$5\nu_1$

Table 3. A comparison of observed and calculated relative intensities for the $n\nu_5$ and $\nu_6 + n\nu_5$ progressions. Note that the n = 4, 5 intensities for the $n\nu_5$ progression are not accurate because of overlap with $\nu_1 + \nu_6 + n\nu_5$ (n = 0, 1). The parameters associated with the $n\nu_5$ progression are probably more indicative of the intrastate vibronic coupling than are those of $\nu_6 + n\nu_5$ (see text).

n	0	1	2	3	4	5
$n\nu_5$						
I (Exp.)	1	2.85	3.75	3.25	(2.85)	(2.60)
I (Calc.)	1	2.70	3.64	3.28	2.21	1.20
(P° = 0.9, D_5 = 2.02)						
$\nu_6 + n\nu_5$						
I (Exp.)	1	1.70	1.70	1.10	0.59	0.18
I (Calc.)	1	1.86	1.72	1.07	0.50	0.18
(P°= 0.62, D_5 = 1.40)						

Figure 1. Calculation of relative intensities of a Franck-Condon progression for a three-dimensional harmonic oscillator based on Eq. 9. Curve (a) corresponds to $P^o = 0.5$, (b) to $P^o = 0.85$ and (c) to $P^o = 1$. Note the rapid build-up in the relative intensity as the intensity maximum moves to larger n.

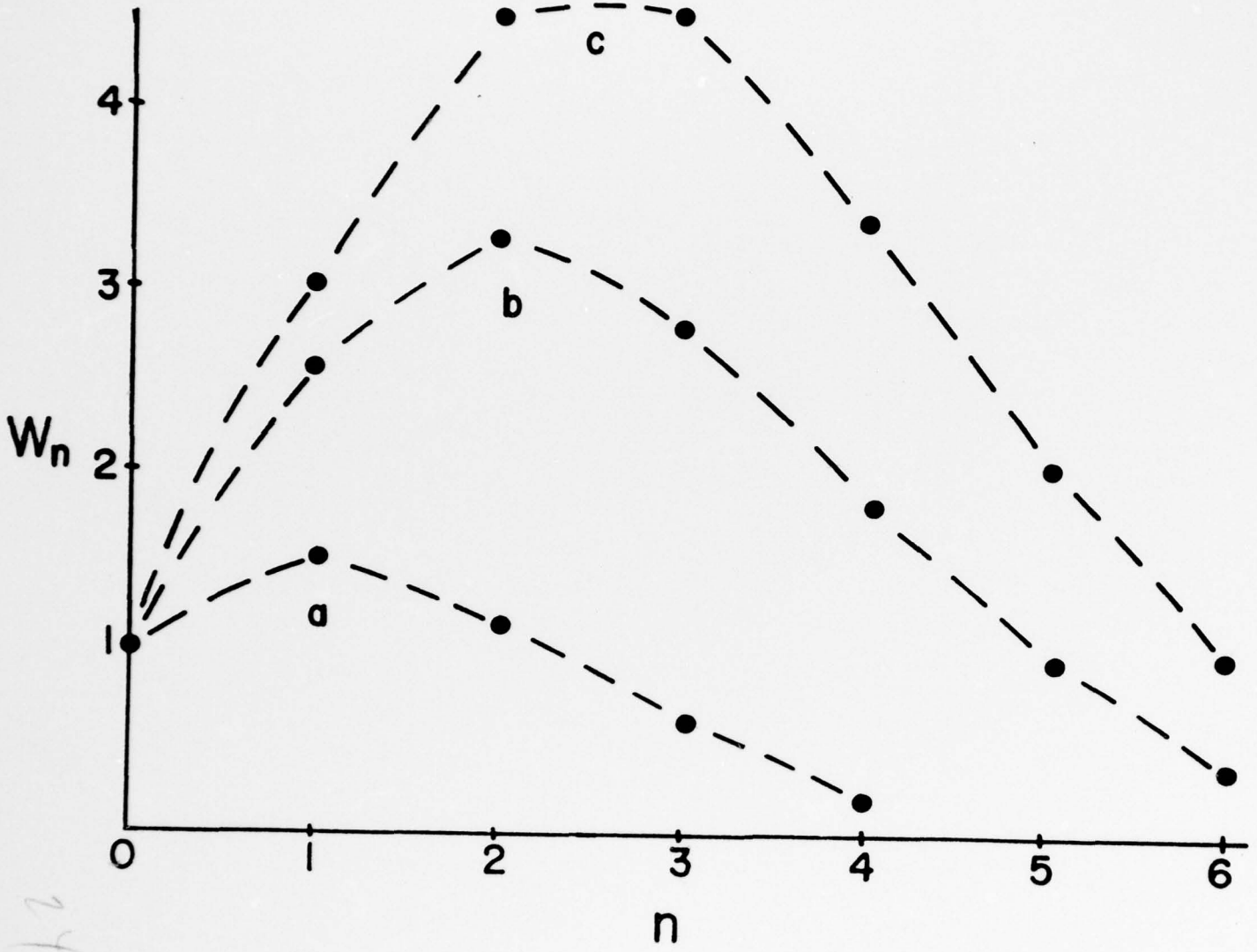
c
b
a
4
3
2
1
W_n
0
1
2
3
4
5
6
n

Figure 2. Comparison of $n\nu_5$ progressions as calculated by the rigorous secular matrix method (10) with one calculated by the approximate method outlined in the text which matches the rigorous curve as closely as possible. Curve (a) was taken from Ref. 10 and has a $D_5 = 2.64$. Curve (b) corresponds to a $D_5 = 2.32$.

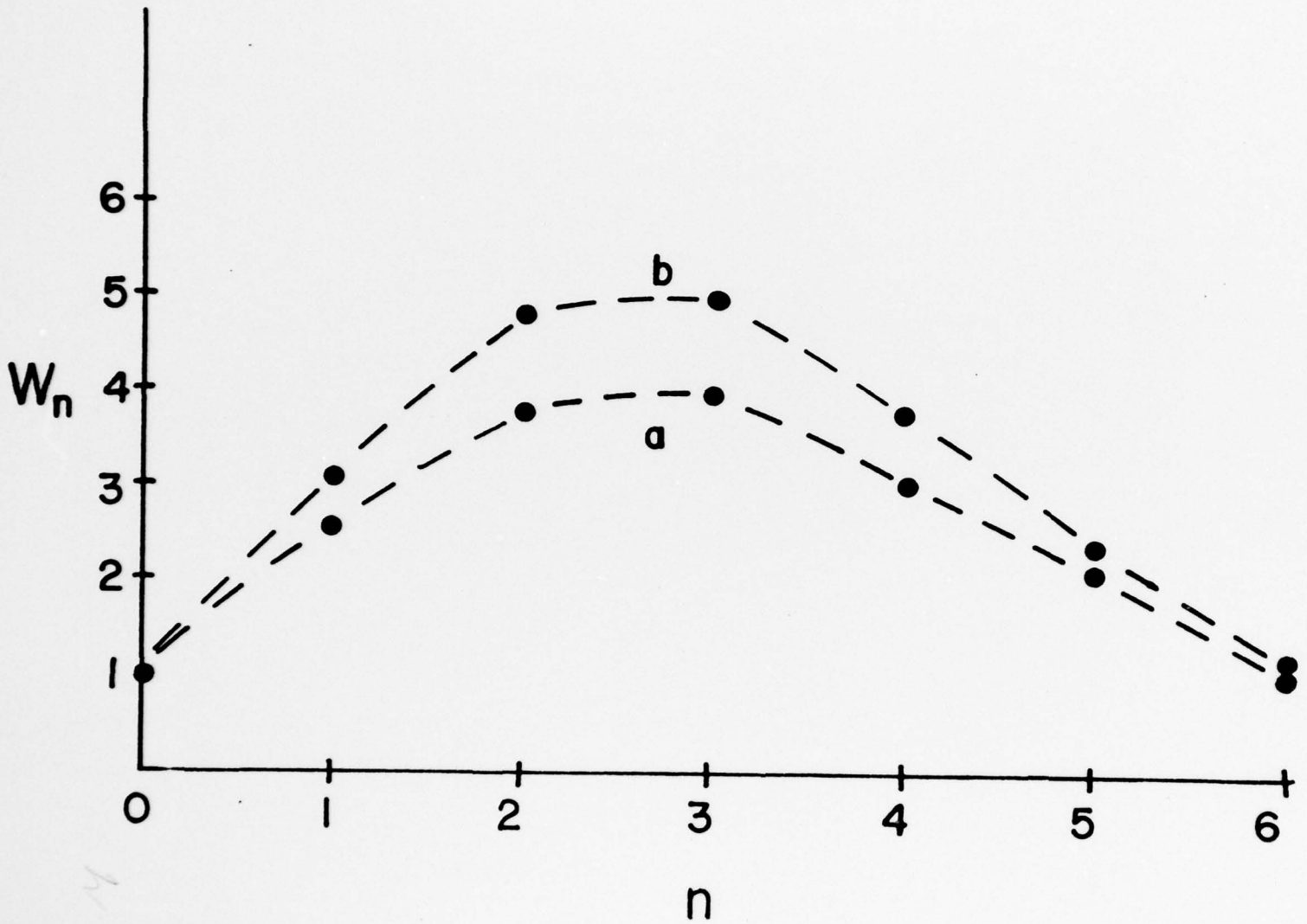
6
5
4
3
2
1
W_n
b
a
0
1
2
3
4
5
6
n

Figure 3. Emission spectrum of 5% UF_6/WF_6 at 1.6 K with .16 Å slits. The curved baseline is an attempt to correct for underlying phonon intensity. The lettered peaks belong to the following ν_5 progressions:

a - $n\nu_5$

b - $\nu_6 + n\nu_5$

c - $\nu_1 + n\nu_5$

d - $\nu_1 + \nu_6 + n\nu_5$

e - $2\nu_1 + n\nu_5$

The unmarked peaks are mainly phonons built on a ν_5 peak.

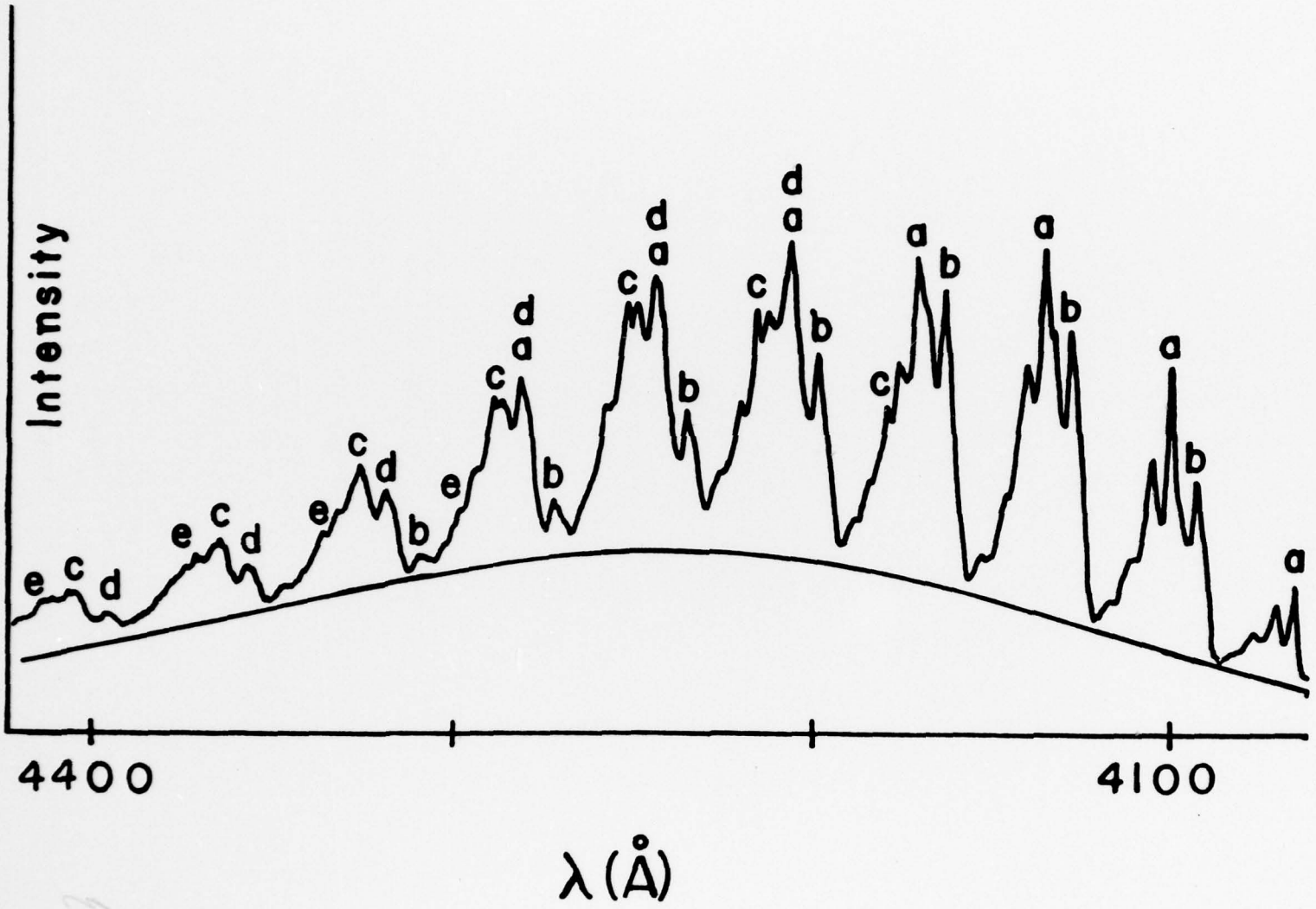
Intensity
4400
4100
λ (Å)

Figure 4. Part of emission spectrum of neat UF_6 at 1.6 K with 0.16 Å slits. Note the broad excitonic band character of many of the peaks.

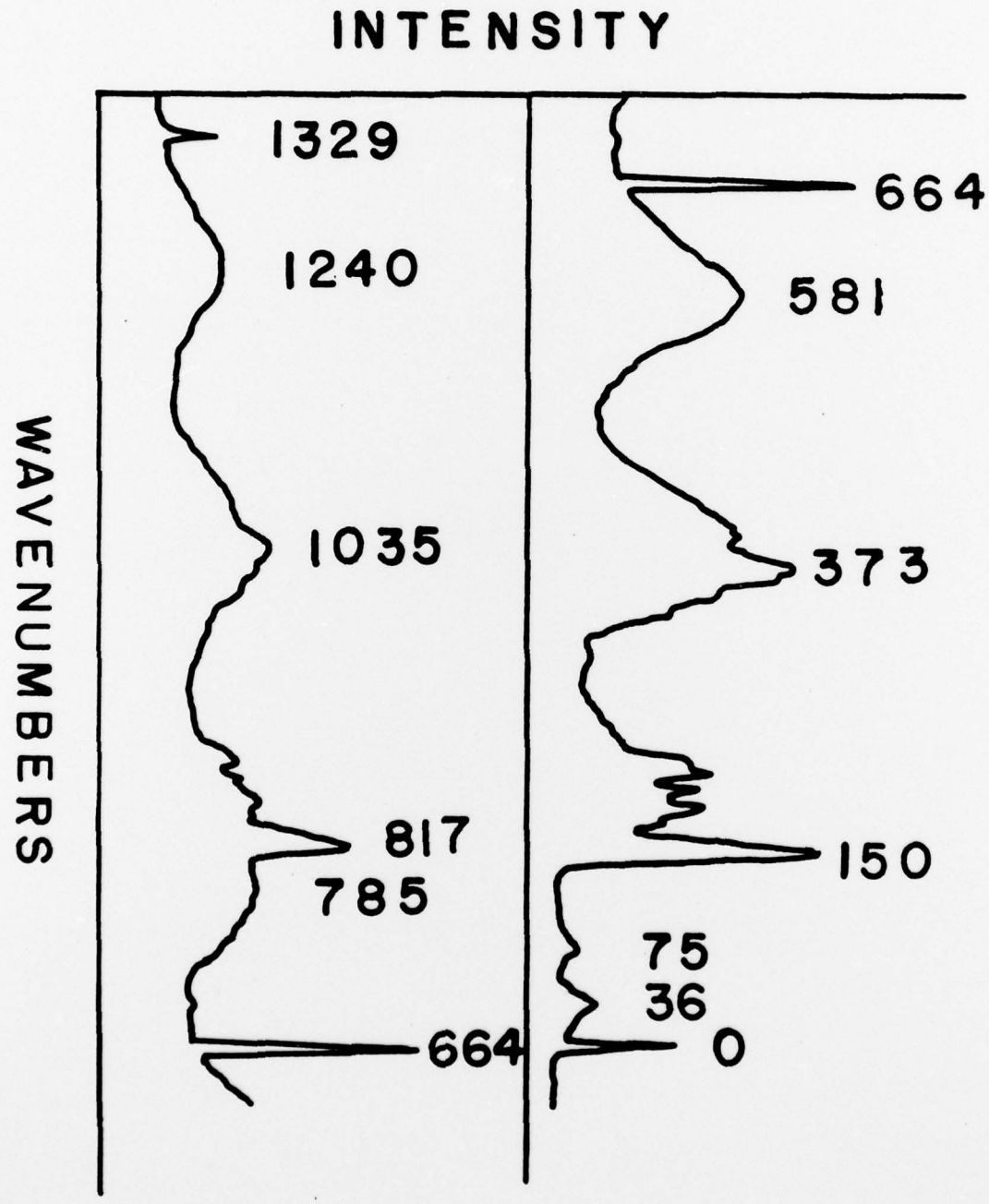
INTENSITY
WAVENUMBERS
1329
1240
1035
817
785
664
664
581
373
150
75
36
0

TECHNICAL REPORT DISTRIBUTION LIST

	No. Copies
Office of Naval Research Arlington, Virginia 22217 Attn: Code 472	2
Office of Naval Research Arlington, Virginia 22217 Attn: Code 102IP 1	6
ONR Branch Office 536 S. Clark Street Chicago, Illinois 60605 Attn: Dr. Jerry Smith	1
ONR Branch Office 715 Broadway New York, New York 10003 Attn: Scientific Dept.	1
ONR Branch Office 1030 East Green Street Pasadena, California 91106 Attn: Dr. R. J. Marcus	1
ONR Branch Office 760 Market Street, Rm. 447 San Francisco, California 94102 Attn: Dr. P. A. Miller	1
ONR Branch Office 495 Summer Street Boston, Massachusetts 02210 Attn: Dr. L. H. Peebles	1
Director, Naval Research Laboratory Washington, D.C. 20390 Attn: Code 6100	1
The Asst. Secretary of the Navy (R&D) Department of the Navy Room 4E736, Pentagon Washington, D.C. 20350	1
Commander, Naval Air Systems Command Department of the Navy Washington, D.C. 20360 Attn: Code 310C (H. Rosenwasser)	1

	No. Copies
Defense Documentation Center Building 5, Cameron Station Alexandria, Virginia 22314	12
U.S. Army Research Office P.O. Box 12211 Research Triangle Park, N.C. 27709 Attn: CRD-AA-IP	1
Naval Ocean Systems Center San Diego, California 92152 Attn: Mr. Joe McCartney	1
Naval Weapons Center China Lake, California 93555 Attn: Head, Chemistry Division	1
Naval Civil Engineering Laboratory Port Hueneme, California 93041 Attn: Mr. W. S. Haynes	1
Professor O. Heinz Department of Physics & Chemistry Naval Postgraduate School Monterey, California 93940	1
Dr. A. L. Slafkosky Scientific Advisor Commandant of the Marine Corps (Code RD-1) Washington, D.C. 20380	1
Office of Naval Research Arlington, Virginia 22217 Attn: Dr. Richard S. Miller	1

TECHNICAL REPORT DISTRIBUTION LIST

	No. Copies
Dr. M. A. El-Sayed University of California Department of Chemistry Los Angeles, California 90024	1
Dr. M. W. Windsor Washington State University Department of Chemistry Pullman, Washington 99163	1
Dr. E. R. Bernstein Colorado State University Department of Chemistry Fort Collins, Colorado 80521	1
Dr. C. A. Heller Naval Weapons Center Code 6059 China Lake, California 93555	1
Dr. M. H. Chisholm Princeton University Department of Chemistry Princeton, New Jersey 08540	1
Dr. J. R. MacDonald Naval Research Laboratory Chemistry Division Code 6110 Washington, D.C. 20375	1
Dr. G. B. Schuster University of Illinois Chemistry Department Urbana, Illinois 61801	1
Dr. E. M. Eyring University of Utah Department of Chemistry Salt Lake City, Utah	1
Dr. A. Adamson University of Southern California Department of Chemistry Los Angeles, California 90007	1
Dr. M. S. Wrighton Massachusetts Institute of Technology Department of Chemistry Cambridge, Massachusetts 02139	1
Dr. M. Rauhut American Cyanamid Company Chemical Research Division Bound Brook, New Jersey 08805	1